2.5D MHD simulation of flux rope formation and eruption driven by converging motion

Xiaozhou Zhao[1,2], Chun Xia [2], Rony Keppens[2], Weiqun Gan[1]

[1] *Key Laboratory of Dark Matter and Space Astronomy, Purple Mountain Observatory, Chinese Academy of Sciences, Nanjing, China.*

[2] *Centre for mathematical Plasma Astrophysics, Department of Mathematics, KU Leuven, Celestijnenlaan 200B, 3001 Leuven, Belgium.*

Abstract

A twisted magnetic flux rope embedded in the lower corona is thought to be a frequent ingredient of a coronal mass ejection(CME). We wish to study in a chromosphere-transition region-corona setup how a magnetic flux rope is formed, and evolves into the corresponding structure of a CME. We study the formation, evolution, and eruption of a magnetic flux rope by 2.5 dimensional resistive MHD simulation. We adopt an initial arcade-like linear force-free configuration in a rectangular simulation box, and drive the system by imposing slow motions which converge towards the magnetic inversion line on the bottom boundary. The convergence imposed to the footpoints of the magnetic arcades brings opposite-polarity magnetic flux to the polarity inversion. After a phase of quasi-static evolution, the convergence gives rise to the formation of a twisted flux rope by magnetic reconnection and finally to the eruption of a CME. In the eruptive phase, the closed magnetic field is severely stretched, leading to the formation of a current sheet, and this in turn enables fast reconnection. We observe the internal structure of the current sheet formed during the eruption process in our simulation. We confirm that the converging flow is a potential mechanism for the formation of magnetic flux ropes, and a possible triggering mechanism for CMEs when a realistic atmosphere is included. Our simulation covers a wide range of scales, from the small-scale current sheet structure to the global-scale magnetic disruption, achieved by the use of the adaptive mesh refinement technique.

Introduction

Flares, coronal mass ejections (CMEs) and eruptive prominences (or filaments) are usually associated in many cases, thus a self-consistent unified model linking these energetic phenomena should be considered.

Because of the rapid development of the magnetic reconnection theory, significant improvements have been made to the "standard" CSHKP senario of flare (e.g., see Benz 2008) since

Kopp and Pneuman (1976). Many theories have been proposed to determine the detailed mechanisms for reconnection (for a review, see e.g., Priest & Forbes 2000). Both observations (e.g., Karlický & Kliem 2010) and simulations (e.g., Ni et al. 2012a; Guidoni et al. 2016) show the processes of the fragmentation of a current sheet, the formation of multiple magnetic islands of different sizes, and the coalescence of plasmoids in unsteady reconnection.

In the solar eruptive process, a current sheet develops between the flare arcade and the CME (Forbes & Acton 1996). CMEs are large-scale energetic phenomena in the solar corona, accompanied by drastic energy release and characterized by mass and magnetic flux ejecting processes. It is believed that a helical magnetic flux rope (FR) buried in the low corona is such an ideal model for the CME progenitor.

Most CME models require the existence or formation of a FR (e.g., Forbes 2000). It is still a debatable question about the formation processes of FRs on the Sun. Two hypotheses have been formulated for the formation of the FRs, i.e., FR emergence from the convection zone and FR formation as a result of photospheric motions.

In this study, we focus on FR formation and eruption, and energy accumulation and dissipation driven by photospheric converging motion, more specifically, an FR is formed at first, then erupts. The relevant prominence formation, flare, CME and reconnection processes were investigated in our study. We studied the formation and eruption processes of FR driven by photospheric converging motion in a chromosphere-transition-corona setup, accounting for the effects of radiative cooling, thermal conduction, gravitational stratification, resistivity and viscosity. Current sheet fragmentation and magnetic islands contraction were also observed in our simulation. Our simulation covers the complete process from FR formation to CME initiation, including the energy accumulation part and dissipatition part.

Numerical Setups

The MHD simulations presented here are performed in a rectangular, Cartesian geometry, ignoring the curvature of the solar surface and the variation of physical variables along z-direction. The evolution of the system can be adequately described by a 2.5D thermodynamic MHD model including gravity, heat conduction, radiative cooling, heating terms, viscosity and resistivity. The energy equation reads

$$\frac{\partial e}{\partial t}+\nabla\cdot((e+p+\frac{1}{2}\mathbf{B}^2)\mathbf{v})=\rho\mathbf{g}\cdot\mathbf{v}+\nabla\cdot(\kappa\cdot\nabla T)-Q+H+(\nabla\cdot\tau)\cdot\mathbf{v}+\eta\mathbf{J}^2. \quad (1)$$

Here, τ is the viscous stress tensor, and η is resistivity. Other quantities, the dimensionless factors of the equations, and the initial conditions of the system now adopt the same setups

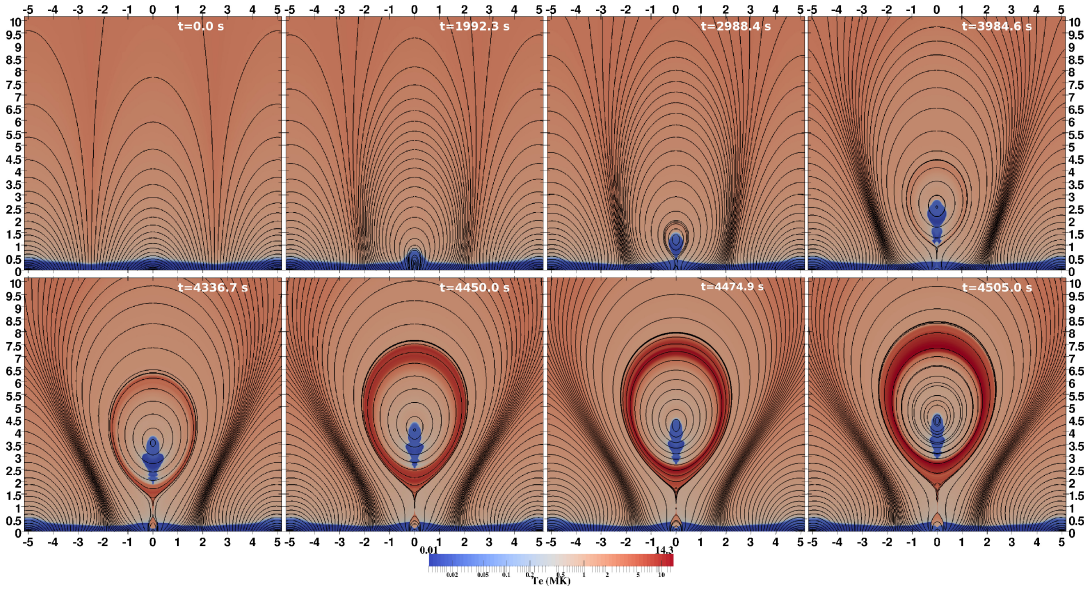

Figure 1: Evolution of temperature with magnetic field lines (solid black lines) overlaid on it.

as Fang et al. (2013) with a characteristic magnetic field strength 20 G. The dimensionless viscosity is 0.0002 while the resistivity is given by

$$\eta = \eta_{chro} + \frac{(\eta_{cor} - \eta_{chro})}{2}[\tanh(\frac{y - h_{tr}}{w_{htra}}) + 1], \tag{2}$$

where $\eta_{chro} = 0.002$, $\eta_{cor} = 0.0002$, and $w_{tr} = 0.05$, with all quantities in normalized units.

The computational box is located in the x-y Cartesian plane. The x-axis is parallel to the solar surface, while the y-axis is vertical. The computational domain is $x_{min} < x < x_{max}$ and $y_{min} < y < y_{max}$, where $x_{min} = -10.0, x_{max} = 0.0, y_{min} = 0, y_{max} = 25.0$ with the length unit 10Mm. Using a mirroring boundary condition at x = 0, we obtain a doubled box with an effective domain of $-10 < x < 10$ and $0 < y < 25$. The mirroring boundary condition is also applied to the left side.

We use closed boundary condition at top side. As for the bottom boundary conditions, our boundary motions are chosen to converge toward the inversion line $x = 0$ at the velocity,

$$v_x = \begin{cases} -v_0 \sin(2\pi x / L_a), |x| < L_d \\ 0, |x| > L_d \end{cases}, \tag{3}$$

where $L_d = \frac{L_a}{2}$,$L_a = 50$Mm, v_0 is the amplitude of the driving velocity, and $v_y = v_z = 0$.

The amplitude of the driving velocity v_0 increases linearly from 0 to 6.5km/s, and keeps $v_0 =$ 6.5km/s ever since. The boundary magnetic field is obtained by zero-gradient finite difference extrapolation. The density and pressure are determined by assuming a hydrostatic atmosphere .

Results

As is illustrated in Figure 1, the magnetic fields of opposite polarity are brought to the magnetic inversion line by the photospheric converging motion, which has been reported from many observations (e.g., Kosovichev and Zharkova 2001), then collide in the photosphere or above. Subsequently magnetic reconnection is driven there, leading to the formation of a helical FR which is capable of supporting the prominence plasma. Afterwards, the newly formed FR erupts, and evolves into the corresponding structure of a CME, which takes on the "three-component" morphology, i.e., an inner bright core, a dark cavity, and a bright leading front. As the reconnection proceeds, plasmoids of different scales are produced, contracted and convected away repetitively.

Figure 2 indicates the cusp-like structure observed in our simulation, which was first discovered by Yohkoh (Masuda et al. 1994)

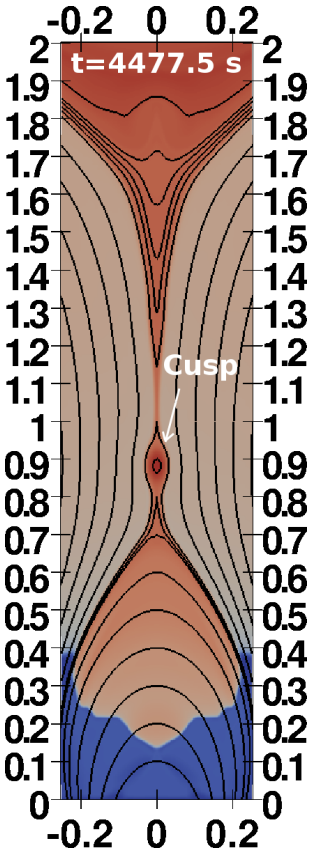

Figure 2: Temperature with magnetic field lines (solid black lines) overlaid on it. The white arrow indicates cusp-like structure.

References

[1] Benz, A. O. 2008, LRSP , 5, 1

[2] Fang, X., Xia, C. & Keppens, R. 2013, ApJL, 771, 2

[3] Forbes, T. G. & Acton, L. W. 1996, ApJ, 459, 330

[4] Forbes, T. G. 2000, J. Geophys. Res., 105, 23153

[5] Guidoni, S. E., DeVore, C. R., Karpen, J. T., & Lynch, B. J. 2016, ApJ, 820, 60

[6] Karlický, M., & Kliem, B. 2010, SoPh , 266, 7

[7] Kopp, R. A., & Pneuman, G. W. 1976, Sol. Phys., 50, 85

[8] Kosovichev, A. G., & Zharkova, V. V. 2001, ApJL , 550, L105

[9] Masuda, S., Kosugi, T., Hara, H., Tsuneta, S., Ogawara, Y. 1994, Natur.371, 495

[10] Ni, L., Roussev, I. I., Lin, J., & Ziegler, U. 2012a, ApJ, 758, 20

[11] Priest, E. R., Forbes, T. G., 2000, Magnetic Reconnection. Cambridge Univ. Press, Cambridge